miR-122 regulation of lipid metabolism revealed by in vivo antisense targeting

Christine Esau,[1,*] Scott Davis,[1] Susan F. Murray,[1] Xing Xian Yu,[1] Sanjay K. Pandey,[1] Michael Pear,[1] Lynnetta Watts,[1] Sheri L. Booten,[1] Mark Graham,[1] Robert McKay,[1] Amuthakannan Subramaniam,[1] Stephanie Propp,[1] Bridget A. Lollo,[1] Susan Freier,[1] C. Frank Bennett,[1] Sanjay Bhanot,[1] and Brett P. Monia[1]

[1] Isis Pharmaceuticals, 1896 Rutherford Road, Carlsbad, California 92008
*Correspondence: cesau@isisph.com

Summary

Current understanding of microRNA (miRNA) biology is limited, and antisense oligonucleotide (ASO) inhibition of miRNAs is a powerful technique for their functionalization. To uncover the role of the liver-specific miR-122 in the adult liver, we inhibited it in mice with a 2′-O-methoxyethyl phosphorothioate ASO. miR-122 inhibition in normal mice resulted in reduced plasma cholesterol levels, increased hepatic fatty-acid oxidation, and a decrease in hepatic fatty-acid and cholesterol synthesis rates. Activation of the central metabolic sensor AMPK was also increased. miR-122 inhibition in a diet-induced obesity mouse model resulted in decreased plasma cholesterol levels and a significant improvement in liver steatosis, accompanied by reductions in several lipogenic genes. These results implicate miR-122 as a key regulator of cholesterol and fatty-acid metabolism in the adult liver and suggest that miR-122 may be an attractive therapeutic target for metabolic disease.

Introduction

MicroRNAs (miRNAs) are a class of endogenously expressed small regulatory noncoding RNAs that are thought to negatively regulate target mRNAs by binding with imperfect complementarity in their 3′UTR (Ambros, 2004; Bartel, 2004; Du and Zamore, 2005; He and Hannon, 2004). Originally identified in *C. elegans* as important for the timing of larval development (Lee et al., 1993), miRNAs have since been implicated in a variety of processes in invertebrates, including cell proliferation, apoptosis, and fat metabolism (Brennecke et al., 2003; Xu et al., 2003). In mammals, only a few miRNAs have been assigned any function, although they are predicted to regulate a large percentage of genes, with estimates based on bioinformatic target prediction ranging as high as 30% (Lewis et al., 2005). Based on the early studies in invertebrates, miRNAs are expected to have similar roles in developmental regulation and cell differentiation in mammals, and roles for miRNAs in cardiogenesis (Zhao et al., 2005) and lymphocyte development (Chen et al., 2004) have been demonstrated. Several studies have also found a strong connection between miRNA and human cancer, including a report that miRNA genes are often found in genomic regions linked to cancer (Calin et al., 2004; McManus, 2003) and a study correlating miRNA expression profiles with developmental lineage and differentiation state of tumors (Lu et al., 2005). A potential role for miRNAs in metabolic pathways has been suggested by studies implicating miRNAs in regulation of adipocyte differentiation (Esau et al., 2004) and glucose-stimulated insulin secretion from pancreatic islet cells (Poy et al., 2004).

miR-122 is expressed in the developing liver (Chang et al., 2004) and at high levels in the adult liver, where it makes up 70% of all miRNA (Chang et al., 2004; Lagos-Quintana et al., 2002). It is one of many tissue-specific microRNAs thought to be important for establishing patterns of gene expression that may be responsible for maintaining the differentiated state of a tissue (Lagos-Quintana et al., 2002; Lim et al., 2005). miR-122 was also reported to enhance replication of HCV through a novel mechanism that is not yet understood, making it a potential therapeutic target for HCV infection (Jopling et al., 2005). Here we report that inhibition of miR-122 in both normal and high-fat-fed mice with a 2′-O-methoxyethyl (2′-MOE) phosphorothioate-modified antisense oligonucleotide (ASO) for over 5 weeks was well tolerated and was associated with a significant reduction in hepatic steatosis and plasma cholesterol levels. These effects were accompanied by a reduction in hepatic sterol and fatty-acid synthesis rates and stimulation of hepatic fatty-acid oxidation. The results suggest that miR-122 may be a therapeutic target for metabolic and cardiovascular diseases.

Results

Modulation of miR-122 activity in vitro with miRNA antisense

In order to monitor ASO inhibition of miR-122, we first confirmed regulation of several computationally predicted miR-122 target genes using a 2′-O-methoxyethyl-phosphorothioate-modified ASO targeting miR-122 in primary mouse hepatocytes in vitro. We have observed improved anti-miRNA activity using 2′-MOE ASO compared to the widely used 2′-O-methyl (2′-OMe) modified ASO (see Figure S1 in the Supplemental Data available with this article online). It is now recognized that miRNAs can cause mRNA degradation of their target genes in addition to translational regulation (Bagga et al., 2005; Lim et al., 2005). Therefore, we monitored mRNA levels of miR-122 target genes predicted by the TargetScan algorithm (Lewis et al., 2003, 2005) using real-time TaqMan RT-PCR following transfection of ASO into primary hepatocytes. Five out of six predicted target mRNAs examined were upregulated 1.5- to 3.5-fold after miR-122 ASO

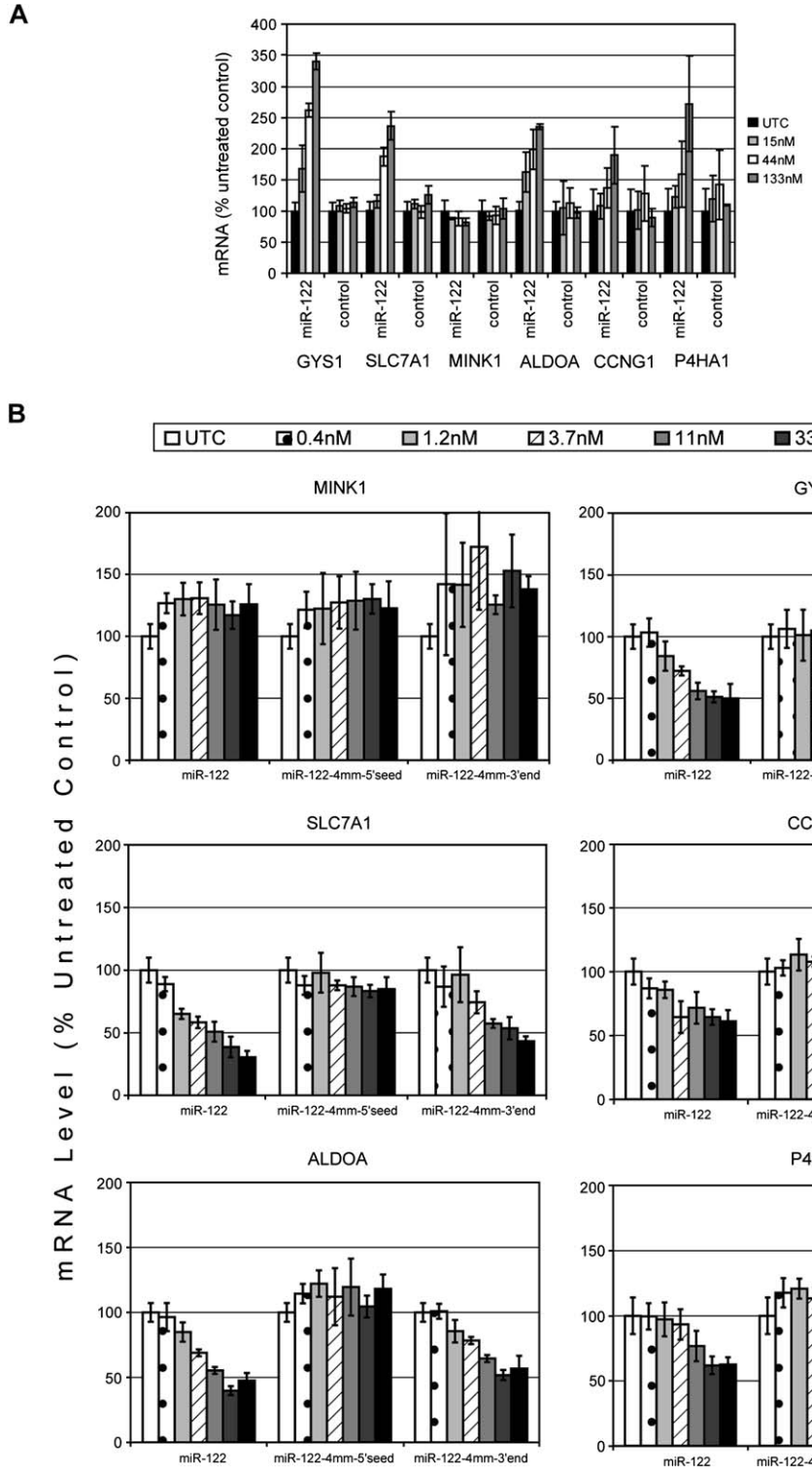

Figure 1. Identification of miR-122 target genes in vitro

A) TaqMan RT-PCR measuring mRNA of predicted miR-122 target genes after transfection of primary mouse hepatocytes with 2′-MOE ASO targeting miR-122 or a control ASO. **B)** TaqMan RT-PCR measuring mRNA of predicted miR-122 target genes after transfection of AML12 with miR-122 duplex RNA or miR-122 duplex RNA with four mismatches in the 5′ seed region or the 3′ half of the miRNA. Error bars represent standard deviation of triplicate samples.

treatment, while none were affected by treatment with an unrelated control ASO (Figure 1A). Only the predicted target *MINK1* was unaffected after miR-122 ASO treatment. To increase our confidence that these target mRNAs were directly regulated by miR-122, a reciprocal experiment was performed in which a miR-122 RNA duplex was transfected into the mouse liver carcinoma AML12 cell line and target mRNA levels were monitored. Although miR-122 is highly expressed in primary hepatocytes, it

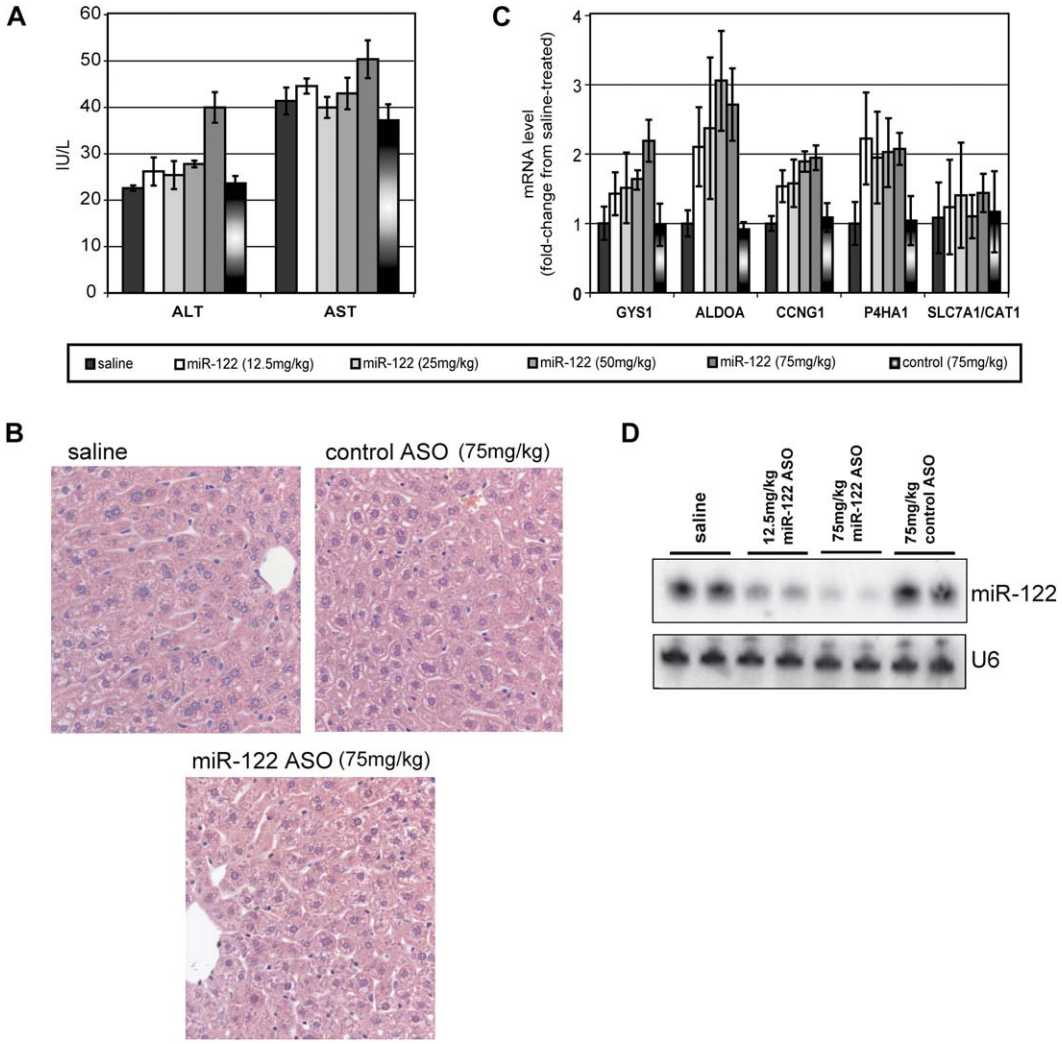

Figure 2. Inhibition of miR-122 in normal mice

Normal mice were treated i.p. with the indicated dose of miR-122 ASO or control ASO twice weekly for 4 weeks. n = 5.

A) Plasma transaminase levels measured at 4 weeks. Error bars = SEM.

B) Representative hematoxylin-and-eosin-stained liver sections from saline- or ASO-treated (75 mg/kg dose) mice, photographed at 40× magnification.

C) TaqMan RT-PCR measuring levels of miR-122 target genes in liver RNA. Error bars = SD.

D) Northern blotting for miR-122 in liver RNA.

is dramatically reduced in most transformed liver cell lines examined, including AML12 cells (Chang et al., 2004). Transfection of miR-122 into AML12 cells led to a decrease in mRNA level for the same five targets that were upregulated by ASO treatment of primary hepatocytes, while *MINK1* was again unaffected (Figure 1B). The interaction of miRNAs with their targets is thought to be primarily mediated through base pairing of the 5′ "seed" portion of the microRNA at positions 2–8 (Lewis et al., 2003, 2005). To demonstrate that regulation of these genes depended on the 5′ seed region of the transfected miRNA, miR-122 with four mismatches in either the 5′ seed sequence or the 3′ portion of the miRNA were also transfected. In agreement with the model for miRNA-target interactions, we found that mutation of the 5′ seed sequence ablated regulation of the target mRNA while mutations in the 3′ half of the miRNA had no effect (Figure 1B). Therefore, these five target mRNAs were regulated by miR-122 in primary hepatocytes in vitro and may be used to monitor antisense inhibition of miR-122 in vivo.

Inhibition of miR-122 in normal mice

We have previously demonstrated that 2′-MOE-modified ASOs are very effective at inhibiting gene expression in liver without further modification or formulation (Yu et al., 2005). Therefore, normal mice were treated intraperitoneally with doses of miR-122 ASO ranging from 12.5 to 75 mg/kg or with 75mg/kg of a control ASO twice weekly for 4 weeks. The mice appeared healthy and normal at the end of treatment, with no loss of body weight or reduced food intake. Plasma transaminase levels were in the normal range (AST $\leq$ 45, ALT $\leq$ 35) for all doses with the exception of the 75 mg/kg dose of miR-122 ASO, which showed a very mild increase in ALT and AST levels (Figure 2A). Histological analysis of liver sections revealed no gross changes in morphology (Figure 2B). To demonstrate the efficacy of the miRNA inhibition, the levels of the five miR-122 target mRNAs identified in cell culture were evaluated in liver by TaqMan RT-PCR (Figure 2C). Four of the five target mRNAs were increased in the miR-122 antisense-treated mice, while no target mRNA changes

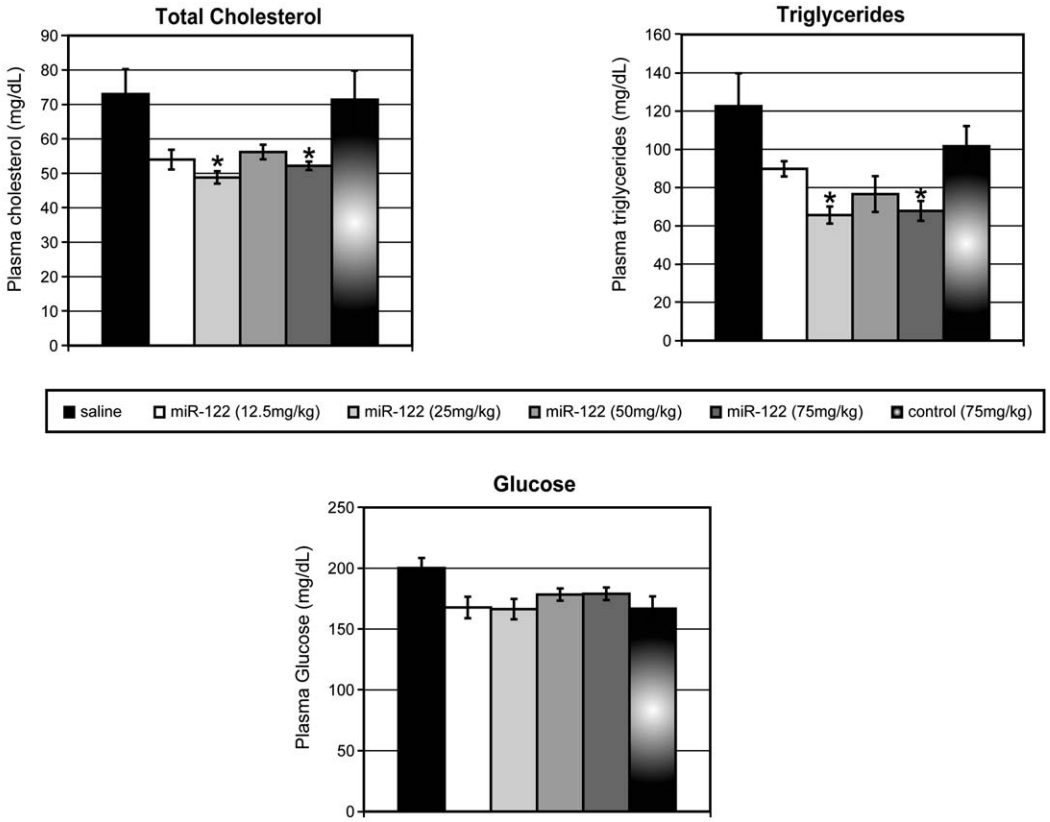

Figure 3. Plasma markers in normal mice after inhibition of miR-122

Plasma cholesterol, triglycerides, and glucose measured in normal mice that had been treated i.p. with the indicated dose of miR-122 or control ASO twice weekly for 4 weeks. n = 5. Error bars = SEM. *$p < 0.05$.

were observed in mice treated with the control ASO, demonstrating specific inhibition of miR-122 activity in liver. In addition, three of the four target mRNAs showed a dose-dependent increase in vivo by miR-122 ASO. *P4HA1* mRNA appeared most sensitive to miR-122 inhibition, as it displayed maximal upregulation at the lowest ASO dose tested.

Northern blotting for miR-122 in liver RNA from these mice revealed a 3-fold reduction in miR-122 level after treatment of mice with the lowest dose of miR-122 ASO, 12.5 mg/kg, when compared to saline-treated mice (Figure 2D). miR-122 levels were reduced more than 10-fold after treatment with the highest dose, 75 mg/kg. The control ASO treatment at the same dose had no effect on miR-122 levels in the liver. A control experiment in which ASO was spiked into liver lysates before RNA preparation confirmed that the reduction of miR-122 signal on the Northern blot was not due to masking of the signal by ASO in the liver RNA preparation (data not shown).

Plasma levels of total cholesterol, triglycerides, and glucose were also monitored. After 4 weeks of ASO treatment, plasma glucose levels were not significantly affected by miR-122 ASO treatment compared to control ASO-treated mice (Figure 3). However, we observed reductions in total cholesterol and triglycerides in the plasma of miR-122 ASO-treated mice at all doses tested, compared to saline or control ASO-treated mice (Figure 3). Total cholesterol was reduced to a similar extent (26%–28%) in mice treated with all doses tested of miR-122 ASO when compared to saline-treated mice.

Microarray analysis of liver gene expression in miR-122 ASO-treated mice

To help elucidate the mechanism of cholesterol lowering caused by miR-122 inhibition in vivo, a cDNA microarray experiment was performed. Liver gene expression was evaluated following 4 weeks of treatment with 50 mg/kg of miR-122 ASO twice weekly and was compared with saline-treated animals (Tables S1 and S2). Analysis of modulated genes by Gene Ontology category revealed that many genes involved in regulation of lipid and carbohydrate metabolism were affected in the ASO-treated mice. Although several genes related to cholesterol metabolism were reduced, only phosphomevalonate kinase mRNA downregulation was statistically significant (Table 1). However, several key genes known to regulate fatty-acid synthesis and oxidation were also downregulated in the microarray experiment and confirmed by RT-PCR, including *FASN*, *ACC1*, *ACC2*, *SCD1*, and *ACLY* (Table 1).

Although the microarray experiment was designed primarily to uncover the downstream effects of miR-122 inhibition after chronic treatment rather than to identify direct miR-122 target genes, we were able to identify 108 significantly upregulated genes with a strict 7 or 8 nucleotide seed match in their 3′UTR (Table S3), which may be direct miR-122 target genes. Most of these mRNAs were modestly increased by only 1.5- to 3-fold, which was similar to the degree of modulation we observed for the target genes identified in cultured hepatocytes after miR-122 ASO transfection.

Table 1. Changes in gene expression after miR-122 ASO treatment of normal mice

	Microarray		RT-PCR	
Gene	Fold Change from Saline	p Value	Fold Change from Saline	p Value
Fatty-Acid Metabolism				
ACACA/ACC1	0.7	0.136	0.7	0.050
ACACB/ACC2	0.4	0.016	0.4	0.002
ACLY	0.3	0.005	0.4	0.002
DGAT1	1.1	0.462	1.1	0.085
DGAT2	0.9	0.384	1.1	0.196
FASN	0.6	0.153	0.6	0.092
LIPC	0.7	0.023	0.8	0.117
PPARGC1A	1.0	0.782	1.1	0.619
PPARA	1.3	0.172	0.9	0.572
SCD1	0.5	0.004	0.2	0.001
SREBP1	0.4	0.004	0.5	0.002
SREBP2	1.0	0.780	0.9	0.016
Cholesterol Metabolism				
CD36	1.4	0.247	0.7	0.014
HMGCR	0.8	0.129	0.8	0.154
LDLR	1.0	0.890	0.9	0.222
PMVK	0.4	0.007	ND	

Liver RNA from mice treated twice weekly for 4 weeks with 50 mg/kg miR-122 ASO or saline was used for a cDNA microarray experiment using GE CodeLink Mouse Whole Genome chips or for TaqMan RT-PCR confirmation of array results. n = 5. Shown are key genes related to lipid metabolism.

Ex vivo analysis of lipid metabolism

The results of the cDNA microarray led us to examine the effect of miR-122 inhibition on the rates of hepatic fatty-acid synthesis and oxidation. Mice were treated with 25 mg/kg miR-122 or control ASO twice a week for 3 weeks. Hepatocytes were then isolated from the treated mice, and the lipid metabolism rates were measured in the cells after overnight culture. In accordance with the observed reduction in *FASN*, *ACC1* and *ACC2* mRNA after miR-122 inhibition, the fatty-acid synthesis rate was reduced and the fatty-acid oxidation rate was increased almost 2-fold in hepatocytes from miR-122 ASO-treated mice compared to saline or control ASO-treated (Figure 4A). The rate of sterol synthesis was also reduced (Figure 4B), which may contribute to the lowered cholesterol levels measured in the plasma of the miR-122 ASO-treated mice. RT-PCR using RNA from the isolated hepatocytes confirmed the reduction in *SCD1* and *ACC2* mRNA in the miR-122 ASO-treated cells (Figure 4C). A reduction in *ACC1* was observed after miR-122 ASO-treatment but was also reduced in the control ASO-treated cells, suggesting that *ACC1* reduction is not responsible for the observed effects on fatty-acid synthesis or oxidation.

Increased fatty-acid oxidation could occur as a result of down-regulation of *ACC2* or an increase in activated AMPK (Hardie, 2003). Therefore, activated (phosphorylated) AMPK levels were also examined by Western blotting of whole liver extracts of mice treated with miR-122 ASO (50 mg/kg twice a week for 4 weeks) and compared to saline- or control ASO-treated mice. Total AMPKα1 protein level was unchanged in the miR-122 ASO-treated mice, but the levels of phosphorylated AMPKα1 were indeed increased more than 2.5-fold compared to saline-treated mice (Figure 4D).

Inhibition of miR-122 in diet-induced obesity mouse model

To further examine the significance of the changes in lipid metabolism observed in normal mice, C57Bl/6 mice that had been fed a high-fat diet for 19 weeks were treated twice a week for 5 1/2 weeks with saline, miR-122 ASO, or control ASO at 12.5 mg/kg, which was the lowest dose tested in the chow-fed mouse study. Upregulation of miR-122 target mRNAs in liver from the miR-122 ASO-treated mice confirmed that miR-122 activity had been effectively inhibited at this dose (Figure 5A). Plasma cholesterol levels were reduced by 35% after two weeks of treatment, and were similarly reduced for the duration of the study. (Figure 5B). Lipoprotein analysis performed using high-performance liquid chromatography showed that the decrease in total cholesterol reflected a reduction in both low-density lipoprotein and high-density lipoprotein fractions (Figure 5C). Consistent with the observed cholesterol reduction, levels of ApoB-100 protein in the plasma of the miR-122 ASO-treated mice were also markedly reduced compared to saline-treated mice, as measured by Western blotting (Figure 5D). ApoB-48 protein was not reduced, however, which is likely due to the fact that the majority of ApoB-48 protein in plasma originates in the intestine rather than the liver (Xie et al., 2003), and miR-122 is not expressed in the intestine (Shingara et al., 2005). Histological analysis of the liver showed substantial reduction of liver steatosis after miR-122 inhibition (Figure 6A), which was also reflected in the reduced levels of triglyceride accumulation in the livers of these mice compared to control ASO-treated (Figure 6A). This was accompanied by a trend toward reduction of plasma transaminase levels in miR-122 ASO-treated mice, indicating an improvement in hepatic function (Figure 6B), although the p value obtained from an analysis of variance was relatively high ($p = 0.1$ for both AST and ALT). As observed in normal mice, these changes also correlated with a reduction in mRNA levels of the same key lipogenic enzymes *FASN*, *ACC2*, and *SCD1* (Figure 6C).

Discussion

Although many miRNAs are ubiquitously expressed, a subset are tissue-specifically expressed during development and are presumed to be important for tissue differentiation. A study examining expression of miRNAs through development in zebrafish found that miRNAs are expressed not early in development but rather after tissue-fate specification, and this study concluded that miRNAs are likely to be more important for later differentiation and maintenance of tissue identity (Wienholds et al., 2005). miR-122 is one such tissue-specific miRNA. It is gradually upregulated in the mouse liver during embryogenesis (Chang et al., 2004) and is likely to regulate aspects of liver development that will eventually be revealed in a germline knockout mouse. The role of miR-122 in the adult liver, however, may be difficult to determine in a knockout mouse, and antisense inhibition is a convenient and effective technique for functionalization of miRNAs in cell culture and in animals (Hutvagner et al., 2004; Krutzfeldt et al., 2005; Meister et al., 2004). In this study, we set out to examine the importance of miR-122 for normal liver function in adult mice by inhibiting miR-122 in vivo with an antisense oligonucleotide. The consequences of inhibiting the most abundant miRNA in the liver were surprisingly mild, given the broad role that miRNAs are expected to play in gene regulation. However, we have uncovered an unexpected role for miR-122 in regulation of hepatic lipid metabolism.

Evidence to date indicates that miRNAs negatively regulate their target mRNAs posttranscriptionally by binding in the 3′UTR.

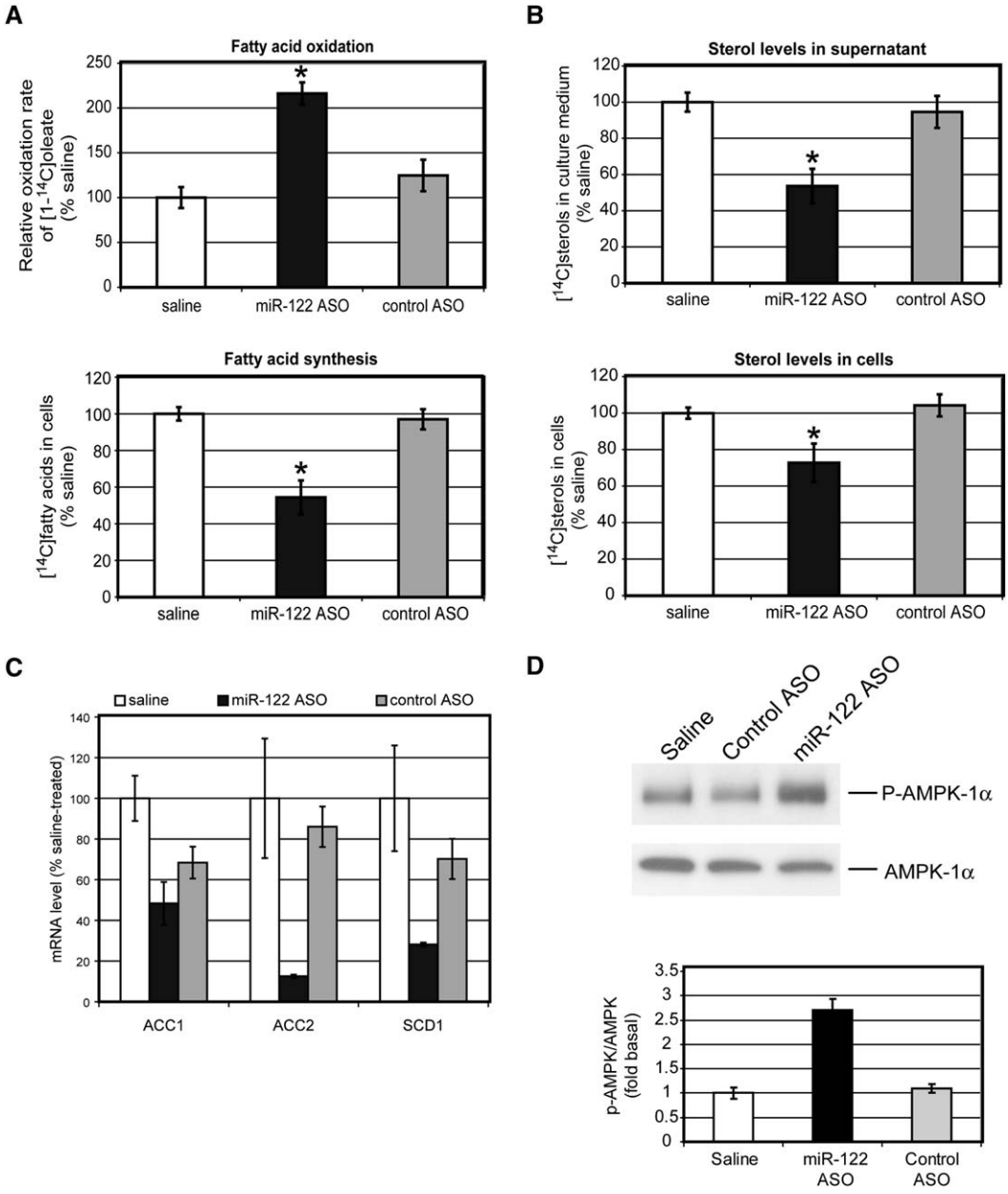

Figure 4. Ex vivo analysis of lipid metabolism after miR-122 inhibition

Hepatocytes isolated from mice treated with miR-122 ASO or a control ASO (25 mg/kg) twice weekly for 3 weeks were used for subsequent in vitro measurement of fatty-acid and sterol synthesis rates and fatty-acid oxidation rates. Shown are results from five mice per group, with each measurement done in triplicate. Error bars = SEM. *$p < 0.05$.

A) Fatty-acid oxidation rate in isolated hepatocytes as measured by oxidation of [1-^{14}C]oleate into $^{14}CO_2$ and [^{14}C]ASPs; de novo fatty-acid synthesis rate as measured by the amount of [^{14}C]acetate incorporated into fatty acids.

B) Sterol synthesis rate in isolated hepatocytes as measured by amount of [^{14}C]acetate incorporated into sterols inside cells or secreted into the culture medium.

C) TaqMan RT-PCR measuring mRNA levels in isolated hepatocytes of genes involved in lipid metabolism.

D) Western blotting for phospho-AMPKα1 catalytic subunit in liver extracts from mice treated with miR-122 ASO or control ASO in vivo twice weekly (50 mg/kg) for 4 weeks. The pictured gel shows pooled samples for each group, but quantitation is from n = 5 samples per group.

The mechanism of downregulation in animals is believed to involve primarily translational repression. However, there is now ample evidence to indicate that miRNA regulation can result in mRNA degradation (Bagga et al., 2005; Lim et al., 2005), possibly by recruiting the mRNA to cytoplasmic sites of mRNA storage and degradation referred to as processing bodies (Liu et al., 2005; Sen and Blau, 2005). We were able to confirm the regulation of several predicted miR-122 target mRNAs by measuring mRNA levels in cell culture and in mice after miR-122 ASO treatment. We did not evaluate translational regulation of the predicted targets, so it is possible that there may be additional translational regulation of other targets such as the predicted target *MINK1*, which did not show any mRNA modulation in response to miR-122 inhibition or addback.

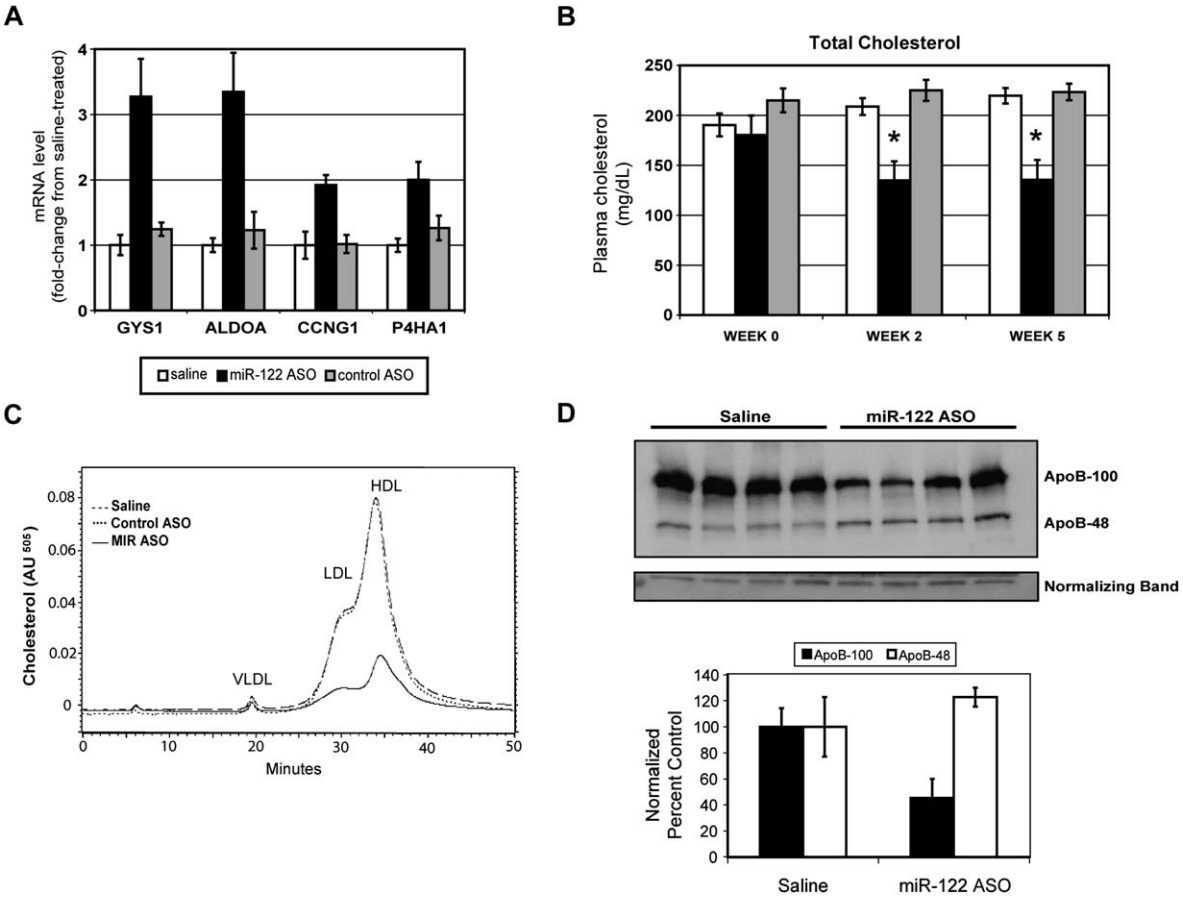

Figure 5. Cholesterol lowering in diet-induced obesity mouse model after miR-122 inhibition

C57Bl/6 mice that had been fed a high-fat diet for 19 weeks were treated s.c. with 12.5 mg/kg miR-122 or control ASO twice weekly for 5 1/2 weeks. n = 5.

A) TaqMan RT-PCR measuring levels of miR-122 target genes in liver RNA after treatement. Error bars = SD.

B) Plasma cholesterol levels at various time points after start of treatment. Error bars = SEM. *$p < 0.05$.

C) High-performance liquid chromatography analysis of lipoprotein profiles in treated mice.

D) Plasma ApoB-100 and ApoB-48 levels measured by Western blotting and normalized to nonspecific band. Graph represents the average of four samples per group with the standard deviation indicated.

Although miR-122 is the most abundant miRNA in hepatocytes, the magnitude of the target mRNA modulation, both in cell culture and in mice, was 1.5- to 3.5-fold. The variation we observed in the dose response to miR-122 ASO treatment in normal mice suggests that each target mRNA may have differential sensitivities to miRNA levels. For example, the target *P4HA1* appeared to be maximally affected even at the lowest ASO dose tested, while regulation of *GYS1* was more dose responsive. We also performed a cDNA microarray experiment that was designed not to identify direct miR-122 target genes but rather to characterize the effect of chronic miR-122 inhibition. Nevertheless, we were able to identify 108 upregulated genes with strict 7 or 8 nucleotide seed matches in their 3′UTR, implicating them as direct miR-122 target genes. Few of these genes were computationally predicted miR-122 targets, suggesting that the current algorithms in use are still insufficient to capture the breadth of miRNA gene regulation. Surprisingly, given the effects we observed on lipid metabolism after miR-122 inhibition, only a few genes known to be involved in lipid metabolism were on this list of potential miR-122 target genes. These putative miR-122 target genes identified by the microarray experiment were also found to be increased by 1.5- to 3-fold. The relationship of miRNA abundance to the magnitude of target modulation or the mechanism (translational repression or mRNA degradation) is not at all understood, but it will be interesting to evaluate whether changes in target mRNA levels will be so easily detectable after inhibition of less abundant miRNAs. Are translational repression and mRNA degradation mutually exclusive outcomes of miRNA regulation, or are they on a continuum, either temporally or relating to the level of miRNA repression?

Given the abundance of miR-122 in the liver, it was expected to play an important role in maintenance of liver differentiation. Surprisingly, the most apparent consequence of miR-122 inhibition in normal mice over 4 weeks was a lowering of plasma cholesterol. The cholesterol lowering was observed in chow-fed mice at a relatively low dose of 25 mg/kg/week miR-122 ASO after 4 weeks, and it was not further improved by higher dosing even though miR-122 levels as measured by Northern blot were more reduced after treatment with a higher dose of ASO. In the high-fat-fed mice, the same 25 mg/kg/week dose of miR-122 ASO caused plasma cholesterol lowering of about 35% compared to saline-treated animals after only 2 weeks of treatment, and treatment for another 3 weeks did not further reduce

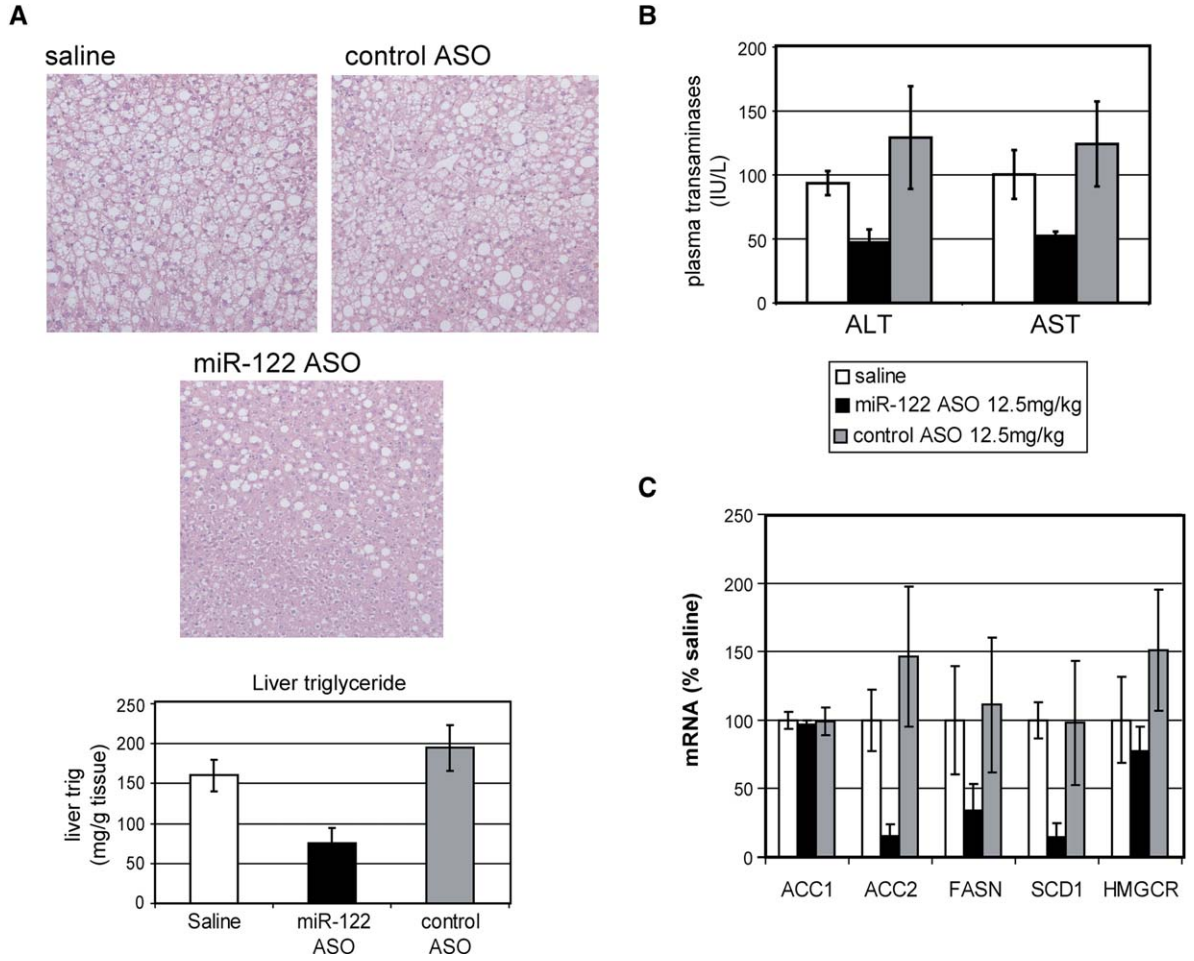

Figure 6. Improvement in liver steatosis in high-fat-fed mice after miR-122 inhibition

C57Bl/6 mice that had been fed a high-fat diet for 19 weeks were treated s.c. with 12.5 mg/kg miR-122 or control ASO twice weekly for 5 1/2 weeks. n = 5. Error bars = SEM.
A) Representative hematoxylin-and-eosin-stained liver sections photographed at 20× magnification and hepatic triglyceride content after 5 1/2 weeks of ASO treatment.
B) Plasma transaminase levels measured after 5 1/2 weeks of ASO treatment.
C) TaqMan RT-PCR evaluating liver mRNA levels of genes involved in lipid metabolism.

cholesterol levels. These data suggest that the cholesterol lowering caused by miR-122 inhibition is not dose-responsively related to the level of inhibition of miR-122. Rather, inhibiting a threshold level of miR-122 results in a change in the steady-state level of plasma cholesterol that does not respond to further inhibition of miR-122. It is likely that this threshold corresponds to the maximal relief from miR-122 regulation of miR-122 target genes responsible for the cholesterol-lowering phenotype. The microarray experiment identified several modulated genes known to be important in cholesterol metabolism, the most prominent being phosphomevalonate kinase (*PMVK*), which was downregulated more than 2-fold in the livers of miR-122 ASO-treated mice. However, this gene is not likely to be a direct miR-122 target as it does not contain a miR-122 seed sequence and is downregulated after miR-122 inhibition. Further work will be required to pinpoint which target genes are responsible for cholesterol lowering.

The decreases in plasma cholesterol observed after miR-122 inhibition reflected reductions in both the high-density and low-density lipoprotein fractions. In mice, unlike in humans, HDL makes up the majority of plasma cholesterol, and one would predict that any drug that significantly lowers total plasma cholesterol levels in mice would have effects on HDL levels. Further experiments in primates or hamsters will be required to evaluate the relative effects of miR-122 inhibition on HDL and LDL in species that have lipoprotein profiles more similar to humans. These will be helpful studies in evaluating the prospects for therapeutically inhibiting miR-122 to lower cholesterol in humans.

The microarray experiment uncovered significant decreases in the mRNA levels of many key genes that regulate lipid metabolism, including *FASN*, *ACC2*, *SCD1*, and *ACLY*. As inhibition of miR-122 is expected to result in upregulation of its direct targets, the exact connection between inhibition of miR-122 and downregulation of these genes is not clear. One possibility is that a transcriptional inhibitor of these genes is negatively regulated by miR-122 and therefore upregulated following miR-122 inhibition, potentially at the level of translation that would not have been identified in the microarray experiment. Also, the effects of depleting a substantial amount of miRNAs in a cell on the activity of other miRNAs have not been explored, but there could be consequences for RISC formation and activity of other miRNAs after miR-122 inhibition. The possibility that miR-122 could be directly downregulating these genes through interaction with their 3′UTRs is not likely, as they do not contain seed

sequences for miR-122, unless the miRNA is acting through a novel mechanism.

From the decreases we observed in the key lipogenic genes after miR-122 inhibition, we would predict profound negative effects on lipogenesis in these animals. Reduction in *ACC* genes, particularly *ACC2*, is expected to cause a decrease in malonyl CoA levels and a subsequent increase in fatty-acid oxidation (Saha and Ruderman, 2003). The result is a switch from an energy-storage to an energy-generating state in the cell. Evaluation of fatty-acid metabolism rates in hepatocytes from miR-122 ASO-treated mice confirmed this. After miR-122 ASO treatment, the hepatic fatty-acid oxidation rate was increased 2-fold compared to saline treatment, and fatty-acid synthesis was down almost 2-fold. The sterol synthesis rate was also down significantly after miR-122 ASO treatment, which is likely at least partially responsible for the plasma cholesterol lowering observed in these mice. These changes in lipid metabolism measured in hepatocytes were also correlated with mRNA reductions in the key genes *ACC2* and *SCD1* that are important for regulation of fatty-acid oxidation and synthesis.

The central metabolic sensor AMPK is a key regulatory enzyme that acts to promote ATP-generating pathways such as fatty-acid oxidation and inhibits energy-storage pathways such as fatty-acid synthesis (Kahn et al., 2005). Because the phenotype that we observed following miR-122 inhibition in mice was consistent with increased AMPK activity, we examined the effect of miR-122 inhibition on this enzyme. Indeed, we found a 2.5-fold increase in the levels of activated AMPK as measured by phosphorylation of the α1 catalytic subunit. However, it is not clear whether AMPK activation is a secondary consequence of miR-122 regulation of other pathways involved in control of lipid metabolism, as a reduction in *SCD1* is sufficient to promote AMPK activation (Dobrzyn et al., 2004). Alternatively, inhibition of miR-122 may first promote AMPK activation through a mechanism still to be determined, which then promotes the switch in energy usage by inhibiting the *ACC2* and *FASN*.

The modulation of lipid metabolism had profound phenotypic effects in the diet-induced obesity mouse model, in which increased fatty-acid oxidation after miR-122 inhibition led to a significant improvement in liver steatosis in addition to cholesterol lowering. These high-fat-fed mice represent a state of prolonged caloric excess, which results in obesity, hyperlipidemia, and hepatic steatosis. An increase in fatty liver has been implicated in the pathogenesis of several metabolic disorders, including nonalcoholic steatohepatitis (NASH) and insulin resistance (Sanyal, 2005). Our data suggest that miR-122 normally plays a significant role in promoting lipid synthesis and inhibiting fatty-acid oxidation in the adult liver and may be a therapeutic target for metabolic and cardiovascular diseases.

During the preparation of this manuscript, Krutzfeldt et al. (2005) reported the inhibition of miR-122 in mice using a cholesterol-conjugated 2′-OMe-modified ASO. Using an acute dosing schedule over 4 days, they demonstrated reduction of miR-122 in the liver and cholesterol lowering in plasma. Although the ASO design and dosing schedules were very different in our respective studies, our results showing cholesterol lowering are in good agreement. Comparing the two microarray experiments, Krutzfeldt et al. identified more changes in genes relating to cholesterol metabolism, which may reflect the earlier time point of their experiment, before compensatory changes in gene expression are seen in the liver in response to lower cholesterol levels. Despite the differences between the experiments, there were many overlapping gene changes (Table S4). In our studies, however, we have extended the analysis of the consequences of miR-122 inhibition to find additional roles for miR-122 in general lipid metabolism.

Inhibition of miR-122 as reported by Krutzfeldt et al. (2005) using the cholesterol-conjugated 2′-OMe ASO involved degradation of the microRNA, which we also observed using an unconjugated 2′-MOE ASO. Although the 2′-MOE ASO was administered at lower doses with a less acute dosing schedule in these studies, it was also effective at miR-122 degradation, target-gene upregulation, and cholesterol lowering in normal mice. This indicates that a conjugation strategy for miRNA-targeting ASOs is not required for effective miRNA inhibition. However, the onset of action of the 2′MOE ASO does appear to be slower, as a similar acute dosing schedule did not produce cholesterol lowering and produced only ~50% reduction of miR-122 (data not shown). Krutzfeldt et al. also reported on the degradation of miR-122 in vivo with the conjugated but not the unconjugated 2′-OMe ASO. We have observed in in vitro experiments that the 2′-MOE-modified ASOs are more effective than 2′-OMe ASOs at inhibiting miRNA activity as measured by a luciferase sensor reporter or a target mRNA in HeLa cells and primary hepatocytes (Figure S1 and data not shown). This may partially explain the ineffectiveness of the unconjugated 2′-OMe ASO at causing miRNA degradation. Krutzfeldt et al. did not report on the ability of the unconjugated 2′-OMe ASO to modulate miR-122 target genes or cause cholesterol lowering, so it is still possible that the unconjugated 2′-OMe ASO can inhibit miRNA activity by sequestering the miRNA without causing degradation.

The results presented here demonstrate that miRNA function can be modulated in rodents using antisense oligonucleotides. Surprisingly, reducing the levels of the most abundant miRNA in the liver by 90% did not produce any untoward effects over a period of 4 weeks. To the contrary, inhibition of miR-122 produced a beneficial effect on plasma cholesterol and hepatic fatty-acid metabolism, improving liver steatosis in a high-fat-fed mouse model. Although much more work is needed to understand all the roles of miR-122 in liver biology and the general role of miRNA in regulation of gene expression, these results portend the therapeutic potential of miRNA modulation.

Experimental procedures

Oligonucleotide synthesis and sequence

Oligonucleotides were prepared using conventional phosphoramidite chemistry and DNA synthesis equipment (ABI). The 2′-O-methoxyethyl phosphoramidites and succinate-linked solid support were prepared as described previously (Martin, 1995). Synthesis of ASOs for animal treatments was as described previously (Cheruvallath et al., 2003). The miR-122 ASO sequence was 5′-ACAAACACCATTGTCACACTCCA-3′. Control ASOs used for cell culture experiments were either a six-mismatch miR-122 ASO of sequence 5′-ACATACTCCTTTCTCAGAGTCCA-3′ or an unrelated control of sequence 5′-CCTTCCCTGAAGGTTCCTCCTT-3′. The unrelated control ASO was used for all animal experiments.

Isolation and transfection of primary mouse hepatocytes and AML12

Primary hepatocytes were isolated from Balb/c mice as previously described (Neufeld, 1997). Cells were seeded into 96-well plates in culture medium (Williams' Medium E supplemented with 10% fetal bovine serum, 10 nM HEPES, and penicillin/streptomycin) and cultured overnight before transfection. Transfection of oligonucleotide in Lipofectin (Invitrogen) was performed in triplicate according to the manufacturer's instructions. Cells were lysed 24 hr after transfection, and total RNA was harvested using QIAGEN RNeasy

96 columns on a Bio Robot 3000 (QIAGEN). Transfection of AML-12 cells with miR-122 duplexed RNA was done using Lipofectamine 2000 (Invitrogen). miR-122 duplex RNA was purchased from Dharmacon. miR-122 duplex: 5′-UGGAGUGUGACAAUGGUGUUUGU-3′ (miR), 5′-AAACACCAUUGUCACACUCCAUA-3′ (complement). 5′mm miR-122: 5′-UGCACAGAGACAAUGGUGUUUGU-3′ (miR), 5′-AAACACCAUUGUCUCUGUGCAUA-3′ (complement). 3′mm miR-122: 5′-UGGAGUGUGACAUUGCAGUAUGU-3′ (miR), 5′-AUACUGCAAUGUCACACUCCAUA-3′ (complement).

Animal care and treatments

All animal experiments were conducted according to the Institutional American Association for the Accreditation of Laboratory Animal Care Guidelines. Male C57BL/6 mice were obtained from The Jackson Laboratory and were housed 4–5 animals per cage with a 12 hr light/dark cycle. Oligonucleotides were dissolved in saline and administered to mice based on body weight by intraperitoneal or subcutaneous injection twice weekly. At study termination, mice were sacrificed in the morning, and liver, kidney, spleen, and epididymal fat pads were removed for further analysis. For diet-induced obesity (DIO) studies, mice were fed a Western diet of 60% lard (Research Diets) for 19 weeks before treatment with oligonucleotide.

Histological analysis

Liver was fixed in 10% buffered formalin and embedded in paraffin wax. Four millimeter sections were cut and mounted on glass slides. After dehydration, the sections were stained with hematoxylin and eosin.

Metabolic measurements

Plasma concentrations of glucose, transaminases, triglycerides, total cholesterol, HDL cholesterol, and LDL cholesterol were determined with an Olympus AU400e automated clinical chemistry analyzer (Melville, NY). Liver triglyceride levels and glycogen contents were analyzed as previously described (Desai et al., 2001).

HPLC analysis of lipoproteins

Serum lipoprotein profiling was performed as described (Kieft et al., 1991) with a Beckman System Gold 126 HPLC system, 507e refrigerated autosampler, 126 photodiode array detector (Beckman Instruments), and a Superose 6 HR 10/30 column (Pfizer). HDL, LDL, and VLDL fractions were measured at a wavelength of 505 nm and validated with a cholesterol calibration kit (Sigma). For each experiment, a three-point standard curve was performed in triplicate to determine the absolute concentration of each lipoprotein fraction.

RT-PCR analysis

Total RNA extracted from whole liver tissue or cultured cells with QIAGEN RNeasy isolation kits was used for real-time quantitative RT-PCR analysis with a Prism 7700 Sequence Detector (Applied Biosystems). mRNA levels were normalized to total RNA for each sample as measured by Ribogreen. All reagents were from Invitrogen. TaqMan primer/probe sequences used for RT-PCR are available on request.

Northern blotting

RNA from livers of treated mice was homogenized in Trizol (Invitrogen) and isolated according to the manufacturer's instructions. Total RNA was separated on a 14% acrylamide TBE 8 M urea minigel containing 20% formamide, then electroblotted onto Hybond N+ nylon filter (Amersham). An end-labeled (Promega) oligonucleotide probe for miR-122 (5′-ACAAACACCATTGTCACACTCCA-3′) was hybridized to the filter in Rapidhyb buffer (Amersham). The blot was reprobed for U6 to control for equal loading. Quantitation was done using a Storm 860 phosphorimager (Molecular Dynamics) and ImageQuant software.

Western blotting

For detection of ApoB levels, plasma diluted 1:80 in lysis buffer (50 mM Tris [pH 7.5], 150 mM NaCl, 1 mM EDTA, 1 mM EGTA, 0.5% NP40, 1% Triton, 0.25% sodium deoxycholate, 0.1% SDS, protease inhibitor cocktail 1:100, 0.2 mM orthovanadate) was electrophoresed on 4%–12% Tris-glycine gels, transferred to PVDF membrane (Invitrogen), and blotted for ApoB-100/-48 with polyclonal antiserum kindly provided by Dr. Stephen G. Young (University of California, Los Angeles). For AMPK and phosphor-AMPK detection, homogenized liver lysates were electrophoresed on a 10% Tris-glycine gel, transferred to PVDF membrane, and blotted for p-AMPK-1α (Cell Signaling) or total AMPK-1α (Upstate Biotechnology). Protein bands were visualized using the ECL Plus Western blot detection kit (Amersham Biosciences) and quantitated using ImageQuant software (Molecular Dynamics).

Microarray

The microarray experiment design was a treatment-control comparison with five mice per group. Liver RNA was isolated from male C57Bl/6 mice injected i.p. 2×/week for 4 weeks with 50 mg/kg miR-122 ASO or saline. RNA from homogenized liver extracts was initially purified by overnight centrifugation after layering onto 5.7 M $CsCl_2$. The pellet was then run through an RNeasy column (Invitrogen) according to the manufacturer's instructions. Microarray analysis was performed by staff at the Biomedical Genomics Laboratory (BIOGEM) at the University of California, San Diego (Dr. Gary Hardiman, Director) using the CodeLink Mouse Whole Genome Bioarray (Amersham-GE). Preparation of the target RNA for hybridization was done as described in Ramakrishnan et al. (2002). Ten micrograms of fragmented target aRNA was used for hybridization to the microarrays. The microarrays were then washed and processed using a direct detection method of the biotin-containing transcripts by a streptavidin-Alexa 647 conjugate as described previously (Ramakrishnan et al., 2002). Processed slides were scanned using an Agilent Microarray Scanner using CodeLink Scanning Software (Motorola Life Sciences) with the laser set to the red dye channel, a Red PMT setting of 70%, and a scan resolution of 5 μm. Images for each slide were quantitated using CodeLink Expression Analysis Software V4.0 (Amersham-GE). Signal intensities for each spot were calculated by summation of the pixel intensities for each spot, then the local background (based on the median pixel intensity of the area surrounding each spot) was subtracted. Whole-array data normalization was performed independently for each slide by dividing each spot's intensity (after background subtraction) by the median signal intensity of all test probes. The resulting data set for each array provided intensities for each probe that were background corrected and normalized to the median intensity of all probes on the array. Pairwise statistical analysis comparing the antisense-treated group with saline control group was performed using Pipeline Pilot (Scitegic, San Diego, CA) and GeneSifter (VisX Labs, Seattle). The median-normalized spot intensities resulting from the CodeLink Analysis Software were log 2 transformed, the mean and standard deviation were calculated, and a two-tailed Student's t test was used to evaluate the significance of changes. During evaluation of the results, data were filtered requiring a p value $< .05$ and a fold change > 1.5 up or down. From this list, associations to NCBI RefSeq sequences were determined from the relationship of CodeLink probes to Entrez Gene entries, then 3′UTR regions excised based on GenBank sequence annotations. This provided 3′UTR sequences for 494 out of 721 probes that were upregulated > 1.5 fold with p value > 0.05.

Determination of sterol and fatty-acid synthesis and fatty-acid oxidation rate

Hepatocytes were isolated as described from male C57Bl/6 mice treated with saline, miR-122 ASO, or control ASO for 3 weeks (25 mg/kg body weight, twice/week for five doses, hepatocyte isolation done 2 days after the last dose). Cells from each animal were plated in triplicate for each assay. For the measurement of sterol and fatty-acid synthesis, 10^6 cells were seeded into each 60 mm plate in supplemented Williams' E medium (10 nM insulin and 10% FBS). After overnight culture, the cells were used for the determination of sterol synthesis and fatty acid synthesis rate by measuring the incorporation of [^{14}C]acetate into sterols and fatty acids, respectively, as described previously (Jiang et al., 2005). For the measurement of fatty acid oxidation rate, 10^6 cells were seeded into each 25 cm^2 flask in supplemented Williams' Medium E. Fatty-acid oxidation rate was evaluated by measuring the oxidation of [1-^{14}C]oleate into $^{14}CO_2$ and acid-soluble products as described (Yu et al., 1997; Yu et al., 2005). Radioactivity levels measured were normalized to total protein for each flask.

Supplemental data

Supplemental Data include one figure and four tables and can be found with this article online at http://www.cellmetabolism.org/cgi/content/full/3/2/87/DC1/.

Acknowledgments

We thank Xiaokun Xiao, Cathie York-DeFalco, and Gene Hung for assistance in histological analysis; Dr. Gary Hardiman and the staff at the UCSD BIOGEM laboratory for microarray service; and Tracy Reigle for assistance with preparing the figures.

Received: November 16, 2005
Revised: January 4, 2006
Accepted: January 10, 2006
Published: February 7, 2006

References

Ambros, V. (2004). The functions of animal microRNAs. Nature *431*, 350–355.

Bagga, S., Bracht, J., Hunter, S., Massirer, K., Holtz, J., Eachus, R., and Pasquinelli, A.E. (2005). Regulation by let-7 and lin-4 miRNAs results in target mRNA degradation. Cell *122*, 553–563.

Bartel, D.P. (2004). MicroRNAs: genomics, biogenesis, mechanism, and function. Cell *116*, 281–297.

Brennecke, J., Hipfner, D.R., Stark, A., Russell, R.B., and Cohen, S.M. (2003). bantam encodes a developmentally regulated microRNA that controls cell proliferation and regulates the proapoptotic gene hid in Drosophila. Cell *113*, 25–36.

Calin, G.A., Sevignani, C., Dumitru, C.D., Hyslop, T., Noch, E., Yendamuri, S., Shimizu, M., Rattan, S., Bullrich, F., Negrini, M., and Croce, C.M. (2004). Human microRNA genes are frequently located at fragile sites and genomic regions involved in cancers. Proc. Natl. Acad. Sci. USA *101*, 2999–3004.

Chang, J., Nicolas, E., Marks, D., Sander, C., Lerro, A., Buendia, M.A., Xu, C., Mason, W.S., Moloshok, T., Bort, R., et al. (2004). miR-122, a mammalian liver-specific microRNA, is processed from hcr mRNA and may downregulate the high affinity cationic amino acid transporter CAT-1. RNA Biol. *1*, 17–24.

Chen, C.-Z., Li, L., Lodish, H.F., and Bartel, D.P. (2004). MicroRNAs modulate hematopoietic lineage differentiation. Science *303*, 83–87.

Cheruvallath, Z., Carty, R., Andrade, M., Moore, M., Song, Q., Rentel, C., Cole, D., and Ravikumar, V. (2003). Efficient synthesis of antisense phosphorothioate oligonucleotides: evaluation of dichloroacetic acid at higher concentration to reduce cycle time. Org. Process Res. Dev. *7*, 917–920.

Desai, U.J., Slosberg, E.D., Boettcher, B.R., Caplan, S.L., Fanelli, B., Stephan, Z., Gunther, V.J., Kaleko, M., and Connelly, S. (2001). Phenotypic correction of diabetic mice by adenovirus-mediated glucokinase expression. Diabetes *50*, 2287–2295.

Dobrzyn, P., Dobrzyn, A., Miyazaki, M., Cohen, P., Asilmaz, E., Hardie, D.G., Friedman, J.M., and Ntambi, J.M. (2004). Stearoyl-CoA desaturase 1 deficiency increases fatty acid oxidation by activating AMP-activated protein kinase in liver. Proc. Natl. Acad. Sci. USA *101*, 6409–6414.

Du, T., and Zamore, P.D. (2005). microPrimer: the biogenesis and function of microRNA. Development *132*, 4645–4652.

Esau, C., Kang, X., Peralta, E., Hanson, E., Marcusson, E.G., Ravichandran, L.V., Sun, Y., Koo, S., Perera, R.J., Jain, R., et al. (2004). MicroRNA-143 regulates adipocyte differentiation. J. Biol. Chem. *279*, 52361–52365.

Hardie, D.G. (2003). Minireview: the AMP-activated protein kinase cascade: the key sensor of cellular energy status. Endocrinology *144*, 5179–5183.

He, L., and Hannon, G.J. (2004). MicroRNAs: small RNAs with a big role in gene regulation. Nat. Rev. Genet. *5*, 522–531.

Hutvagner, G., Simard, M.J., Mello, C.C., and Zamore, P.D. (2004). Sequence-specific inhibition of small RNA function. PLoS Biol. *2*, E98. Published online February 24, 2004. 10.1371/journal.pbio.0020098.

Jiang, G., Li, Z., Liu, F., Ellsworth, K., Dallas-Yang, Q., Wu, M., Ronan, J., Esau, C., Murphy, C., Szalkowski, D., et al. (2005). Prevention of obesity in mice by antisense oligonucleotide inhibitors of stearoyl-CoA desaturase-1. J. Clin. Invest. *115*, 1030–1038. Published online March 10, 2005. 10.1172/JCI200523962.

Jopling, C.L., Yi, M., Lancaster, A.M., Lemon, S.M., and Sarnow, P. (2005). Modulation of hepatitis C virus RNA abundance by a liver-specific MicroRNA. Science *309*, 1577–1581.

Kahn, B.B., Alquier, T., Carling, D., and Hardie, D.G. (2005). AMP-activated protein kinase: ancient energy gauge provides clues to modern understanding of metabolism. Cell Metab. *1*, 15–25.

Kieft, K.A., Bocan, T.M., and Krause, B.R. (1991). Rapid on-line determination of cholesterol distribution among plasma lipoproteins after high-performance gel filtration chromatography. J. Lipid Res. *32*, 859–866.

Krutzfeldt, J., Rajewsky, N., Braich, R., Rajeev, K.G., Tuschl, T., Manoharan, M., and Stoffel, M. (2005). Silencing of microRNAs in vivo with ''antagomirs''. Nature *438*, 685–689. Published online October 30, 2005. 10.1038/nature04303.

Lagos-Quintana, M., Rauhut, R., Yalcin, A., Meyer, J., Lendeckel, W., and Tuschl, T. (2002). Identification of tissue-specific microRNAs from mouse. Curr. Biol. *12*, 735–739.

Lee, R.C., Feinbaum, R.L., and Ambros, V. (1993). The C. elegans heterochronic gene lin-4 encodes small RNAs with antisense complementarity to lin-14. Cell *75*, 843–854.

Lewis, B.P., Shih, I.H., Jones-Rhoades, M.W., Bartel, D.P., and Burge, C.B. (2003). Prediction of mammalian microRNA targets. Cell *115*, 787–798.

Lewis, B.P., Burge, C.B., and Bartel, D.P. (2005). Conserved seed pairing, often flanked by adenosines, indicates that thousands of human genes and microRNA targets. Cell *120*, 15–20.

Lim, L.P., Lau, N.C., Garrett-Engele, P., Grimson, A., Schelter, J.M., Castle, J., Bartel, D.P., Linsley, P.S., and Johnson, J.M. (2005). Microarray analysis shows that some microRNAs downregulate large numbers of target mRNAs. Nature *433*, 769–773.

Liu, J., Valencia-Sanchez, M.A., Hannon, G.J., and Parker, R. (2005). MicroRNA-dependent localization of targeted mRNAs to mammalian P-bodies. Nat. Cell Biol. *7*, 719–723.

Lu, J., Getz, G., Miska, E.A., Alvarez-Saavedra, E., Lamb, J., Peck, D., Sweet-Cordero, A., Ebert, B.L., Mak, R.H., Ferrando, A.A., et al. (2005). MicroRNA expression profiles classify human cancers. Nature *435*, 834–838.

Martin, P. (1995). Ein neuer Zugang zu 2′-O-Alkylribonucleosiden und Eigenschaften deren Oligonucleotide. Helv. Chim. Acta *78*, 486–504.

McManus, M.T. (2003). MicroRNAs and cancer. Semin. Cancer Biol. *13*, 253–258.

Meister, G., Landthaler, M., Dorsett, Y., and Tuschl, T. (2004). Sequence-specific inhibition of microRNA- and siRNA-induced RNA silencing. RNA *10*, 544–550.

Neufeld, D.S. (1997). Isolation of rat liver hepatocytes. Methods Mol. Biol. *75*, 145–151.

Poy, M.N., Eliasson, L., Krutzfeldt, J., Kuwajima, S., Ma, X., MacDonald, P.E., Pfeffer, S., Tuschl, T., Rajewsky, N., Rorsman, P., and Stoffel, M. (2004). A pancreatic islet-specific microRNA regulates insulin secretion. Nature *432*, 226–230.

Ramakrishnan, R., Dorris, D., Lublinsky, A., Nguyen, A., Domanus, M., Prokhorova, A., Gieser, L., Touma, E., Lockner, R., Tata, M., et al. (2002). An assessment of Motorola CodeLink microarray performance for gene expression profiling applications. Nucleic Acids Res. *30*, e30.

Saha, A.K., and Ruderman, N.B. (2003). Malonyl-CoA and AMP-activated protein kinase: an expanding partnership. Mol. Cell. Biochem. *253*, 65–70.

Sanyal, A.J. (2005). Mechanisms of Disease: pathogenesis of nonalcoholic fatty liver disease. Nat. Clin. Pract. Gastroenterol. Hepatol. *2*, 46–53.

Sen, G.L., and Blau, H.M. (2005). Argonaute 2/RISC resides in sites of mammalian mRNA decay known as cytoplasmic bodies. Nat. Cell Biol. *7*, 633–636.

Shingara, J., Keiger, K., Shelton, J., Laosinchai-Wolf, W., Powers, P., Conrad, R., Brown, D., and Labourier, E. (2005). An optimized isolation and labeling platform for accurate microRNA expression profiling. RNA *11*, 1461–1470. Published online July 25, 2005. 10.1261/rna.2610405.

Wienholds, E., Kloosterman, W.P., Miska, E., Alvarez-Saavedra, E., Berezikov, E., de Bruijn, E., Horvitz, R.H., Kauppinen, S., and Plasterk, R.H. (2005). MicroRNA Expression in Zebrafish Embryonic Development. Science *309*, 310–311. Published online May 26, 2005. 10.1126/science.1114519.

Xie, Y., Nassir, F., Luo, J., Buhman, K., and Davidson, N.O. (2003). Intestinal lipoprotein assembly in apobec-1/ mice reveals subtle alterations in triglyceride secretion coupled with a shift to larger lipoproteins. Am. J. Physiol. Gastrointest. Liver Physiol. *285*, G735–G746.

Xu, P., Vernooy, S.Y., Guo, M., and Hay, B.A. (2003). The Drosophila microRNA Mir-14 suppresses cell death and is required for normal fat metabolism. Curr. Biol. *13*, 790–795.

Yu, X.X., Drackley, J.K., and Odle, J. (1997). Rates of mitochondrial and peroxisomal beta-oxidation of palmitate change during postnatal development and food deprivation in liver, kidney and heart of pigs. J. Nutr. *127*, 1814–1821.

Yu, X.X., Murray, S.F., Pandey, S.K., Booten, S.L., Bao, D., Song, X.Z., Kelly, S., Chen, S., McKay, R., Monia, B.P., and Bhanot, S. (2005). Antisense oligonucleotide reduction of DGAT2 expression improves hepatic steatosis and hyperlipidemia in obese mice. Hepatology *42*, 362–371.

Zhao, Y., Samal, E., and Srivastava, D. (2005). Serum response factor regulates a muscle-specific microRNA that targets Hand2 during cardiogenesis. Nature *436*, 214–220.

Accession numbers

The microarray data described herein are deposited at NCBI GEO (http://www.ncbi.nih.gov/geo) with accession series GSE3603.